Available online at www.sciencedirect.com
ScienceDirect
International Journal of Heat and Mass Transfer 50 (2007) 3359–3365
International Journal of HEAT and MASS TRANSFER
www.elsevier.com/locate/ijhmt

Combustion of suspended fine solid fuel in air inside inert porous medium: A heat transfer analysis

Tarun K. Kayal *, Mithiles Chakravarty

Chemical Engineering Section, Central Glass and Ceramic Research Institute, Kolkata 700 032, India

Received 20 March 2006; received in revised form 19 January 2007
Available online 2 April 2007

Abstract

Present work is a numerical analysis of combustion of submicron carbon particles inside an inert porous medium where the particles in form of suspension in air enter the porous medium. A one-dimensional heat transfer model has been developed using the two-flux gray radiation approximation for radiative heat flux equations. The effects of absorption coefficient, emissivity of medium, flame position and reaction enthalpy flux on radiative energy output efficiency have been presented. It is revealed that in porous medium the combustion of suspended carbon particles is similar to premixed single phase gaseous fuel combustion except the former has shorter preheating temperature zone length. Use of porous ceramic having high porosity and made of Al_2O_3 or ZrO_2 with stabilized flame position operated nearer to downstream end will ensure radiative output maximum and minimum at downstream and upstream end, respectively.

Keywords: Solid particle combustion; Inert porous medium; Heat transfer; Radiation; Modeling

1. Introduction

In recent years, the development of porous radiant burner concept for gaseous fuels has also taken new dimension due to its several advantages over the free flame burners. In a porous burner, combustion of premixed gaseous fuel-air mixture inside the porous matrix releases energy to heat up the matrix which converts sensible heat of combustion gas to radiative energy. The radiative energy, apart from preheating the gas-air mixture for combustion augmentation, is emitted at the downstream end to heat up the load. In comparison to conventional burners, the porous gas burners have higher thermal efficiency, high power density, low emission of CO and NO_x and better flame stability. Various thermal applications in both domestic and industrial sector have been reported [1,2].

Elaborate analytical and experimental studies have been made to analyze the combustion characteristics of porous medium burner for gaseous fuel-air mixture system [3–7]. Limited number of experimental and numerical studies have been reported for combustion of liquid fuel using porous medium [8–13]. In these studies, the oil was fed in form of oil spray or drops in air at the entry point and the vaporization of oil occurs with the upstream radiative heat before combustion of oil vapor-air mixture within the porous matrix. Fuse et al. [14] used the upstream radiative heat from the combustion of oil in the matrix and furnace wall to vaporize the oil from oil container for sustained oil vaporization and stable combustion. Kayal and Chakravarty [15] developed a two-dimensional model based on a conceptual system where the liquid fuel is vaporized through indirect heat transfer from vaporized fuel combustion zone. The vaporization energy has been derived through radiative interaction of the vaporizing plate and an upstream end surface of the porous medium. The medium converts the sensible heat of the combustion gas to downstream radiative heat flux. Emmisivities of vaporizing plate and porous medium along with optical thickness of medium affect the radiative output of the system significantly. Several experimental studies have been made [16–18] on the combustion behavior

* Corresponding author.
E-mail address: tarun@cgcri.res.in (T.K. Kayal).

0017-9310/$ - see front matter © 2007 Elsevier Ltd. All rights reserved.
doi:10.1016/j.ijheatmasstransfer.2007.01.041

Nomenclature

a	specific area, m^{-1}
a^*	absorption coefficient of porous medium, m^{-1}
$a^{*\prime}$	effective absorption coefficient of region A, m^{-1}
b	enhancement factor of absorption coefficient, $a^{*\prime}/a^*$
c	specific heat of mixture at constant pressure, J kg^{-1} K^{-1}
d	carbon particle diameter, m
E^*	emissivity of inert solid medium
E'	downstream radiative efficiency in percent, $q^*(L)$ q'^{-1}
E''	total radiative efficiency in percent, $[q^*(L) - q^*(0)]/q'$
f	equivalence ratio
h	heat transfer coefficient, W m^{-2} K^{-1}
i	radiation intensity, W m^{-2}
i_b	black body intensity, W m^{-2}
k	thermal conductivity, W m^{-1} K^{-1}
L	porous layer length, m
L'	dimensionless preheating temperature zone length, $(x^* - x')/L$
m	mass of single carbon particle, kg
M	molecular weight, kg mol^{-1}
M_1, M_2, M_3	dimensionless quantities as in Eq. (11)
n	number density of carbon particles, m^{-3}
p	pressure, N m^{-2}
q	radiative heat flux, W m^{-2}
q^*	net radiative heat flux, W m^{-2}
q'	reaction enthalpy flux, W m^{-2}
Q	dimensionless radiative heat flux, $q\sigma^{-1}T_i^{-4}$
Q^*	dimensionless net radiative heat flux, $q^*\sigma^{-1}T_i^{-4}$
Q'	dimensionless reaction enthalpy flux, $q'\sigma^{-1}T_i^{-4}$
R	universal gas constant, J mol^{-1} K^{-1}
s	scattering coefficient, m^{-1}
s_1, s_2	scattering coefficient of region C and A, respectively, m^{-1}
T	temperature, K
T_A	autoignition temperature, K
T^*	dimensionless temperature, $(T_g - T_i)/T_i$
$T^{*\prime}$	dimensionless peak gas temperature, $(T_m - T_i)/T_i$
T_A^*	dimensionless autoignition temperature, $(T_A - T_i)/T_i$
u	axial velocity, m s^{-1}
u_f	laminar flame burning velocity of carbon dust at stoichiometric dust concentration in air, m s^{-1}
V^*	dimensionless burning velocity, u_3/u_1
x	axial coordinate, m
x^*	axial coordinate at flame plane, m^{-1}
x'	value of x at $T^* = 0.01$
X^*	dimensionless axial coordinate in flame plane, x^*L^{-1}
X	dimensionless axial coordinate, xL^{-1}
y	mass fraction of gaseous product

Greek symbols

α	absorption coefficient, m^{-1}
φ	porosity
ρ	density, kg m^{-3}
σ	Stefen–Boltzman constant, W m^{-2} K^{-4}
ψ	inertial impact factor
λ	cross sectional area ratio of solid with and without suspended carbon particles

Superscripts

+	forward direction
−	backward direction

Subscripts

e	exit plane
g	gas
gc	between gas and carbon particle
gs	between gas and solid medium
i	inlet plane
m	maximum
s	solid medium
1, 2, 3, 4	interfacial plane

of kerosene when kerosene oil was added dropwise at the top of the ceramic porous matrix. The oil got vaporized during its downward passage inside the porous media and had combustion after mixing with air inside the matrix. Kayal and Chakravarty [19] presented numerical analysis of combustion of liquid fuel oil where the oil flows under gravity through an inert porous medium wetting its solid wall with con- current movement of liquid fuel and air under steady state conditions. The effects of various properties of porous medium and operating parameters on the vaporization zone and radiation energy output have been discussed. Non-isothermal plug flow of pulverized bituminous coal suspension has been used to estimate and verify experimentally data regarding various involved operations upto combustion of individual coal particles [20]. Three-dimensional computational fluid dynamics have been carried out extensively for boilers using pulverized coal [21]. In recent years, the focus is on utilization of various waste materials in conjunction with conventional fuel for combustion in fluidized bed or in form of pulverized particles. Bubbling fluidized bed combustion of coal, biomass, agricultural waste, industrial waste has been studied experimentally with theoretical model recently [22]. Fluidized combustion of municipal solid waste and lignite has also been studied [23]. Coal combustion behavior has been studied [24] using semi-empirical model in estimating particle size distribution in a circulating

fluidized bed where both axial and radial segregation of coal particles were considered. Experimental and theoretical study of combustion of coal reburn with natural gas in pulverized fuel combustion was made for predicting NO_x emission [25]. No numerical and experimental study of combustion of pulverized fuel in inert porous medium has been reported so far. The present study investigates numerically the thermal behavior of a highly porous ceramic matrix for combustion of submicron carbon (carbon black) particles suspended in air.

2. Mathematical analysis

2.1. Analytical model

The schematic diagram representing one-dimensional model under steady state condition is shown in Fig. 1. A uniform suspension of carbon (carbon black) particles in air with mass velocity ρu in laminar flow enters an adiabatic duct containing inert porous medium of length L. The particle laden air enters medium ($x = 0$) at temperature T_i, burns near the region at $x = x^*$ and flows out at $x = L$ at temperature T_e. The porous medium is divided into three regions A, B and C. The interfacing planes which are perpendicular to x-direction are separating the regions and designated by 1, 2, 3 and 4. The radiative heat fluxes in forward and backward in the porous medium are q^+ and q^-, respectively.

The principal assumptions used in the formulation are as follows:

a) The working gas is non-radiating as the emissivity of gas is much less than that of porous material.
b) The pressure drop across the porous media is negligible due to laminar flow of gas through highly porous structure. This is justified as the usual matrix structure [6] of radiant burners is in the form of open cellular foams or ceramic fiber structure having porosity in the range of 0.95–0.99.
c) The porous medium and the carbon particles are able to emit and absorb radiation in local thermal equilibrium while radiative scattering is ignored. This assumption is realized to cover most of porous medium such as ceramic foam [5] and porous metallic structure [3].
d) The porous medium is a homogeneous continuum, the physical properties of which are given by multiplying those of porous material by a factor of $(1 - \varphi)$.
e) In precombustion region A, the presence of carbon particles leads to increase in effective absorption coefficient of matrix a few fold. This assumption is realized as the increase of absorption coefficient has been observed for ceramic matrix [7,26] and metallic wire mess structure [17,27] when the porosity of structure decreases in both cases. For ceramic foam structure (PSZ) of 10 and 65 ppi (pores per inch), the porosities of matrix are 0.87 and 0.84 and absorption coefficients (1/m) are estimated to be 72 and 250–750, respectively [26]. In the present study, the effective porosity of solid for flow of gas decreases from 0.95 to 0.873 due to presence of carbon particles in the voids of matrix for stoichiometric carbon loading in air. So the presence of carbon particles leads to significant increase in absorption coefficient in the precombustion zone A. However, no mathematical correlation between porosity and absorption coefficient has been reported so far.
f) A one-dimensional radiative propagation occurs in x-direction without any reaction being taken place in region A and C. This assumption is reasonable due to high thermal insulation outside the duct in presence of negligible radial flow.
g) Physical interaction between porous medium surface and suspended carbon particles in air stream in region A is negligible. For ceramic foams with high porosity i.e. low number of pores per inch, the collecting structure of porous medium [14,26] for solid carbon particles in air is between 1.5 and 2.5 mm. Inertial impaction factor (ψ) based on Stokes law for cylindrical targets on the suspension flow of carbon black particles in the size range of 28–500 nm [28] has been estimated [29]. Corresponding inertial impact collection efficiency of target is nearly nil [29], confirming no interaction between flowing particles with porous structure.
h) No temperature gradient exists inside each solid particle as Biot number $[hd/k_s]$ is estimated to be much less than 0.1 for fine particles [30].
i) The porous medium is non-catalytic.
j) The suspension of particles in air enters the region at a temperature $T_g \leqslant T_A$ where T_A is the autoignition temperature of carbon black-air suspension. The maximum temperature of carbon particle-air suspension is the autoignition temperature, T_A before it enters the reaction region B. However, gas entry temperature T_2 for methane combustion in porous matrix was obtained to be less than T_A [3].
k) The oxidation reaction of carbon particles starts and gets completed at constant temperature $T_g = T_m$. As the porosity of solid medium is very high ($\varphi > 0.9$)

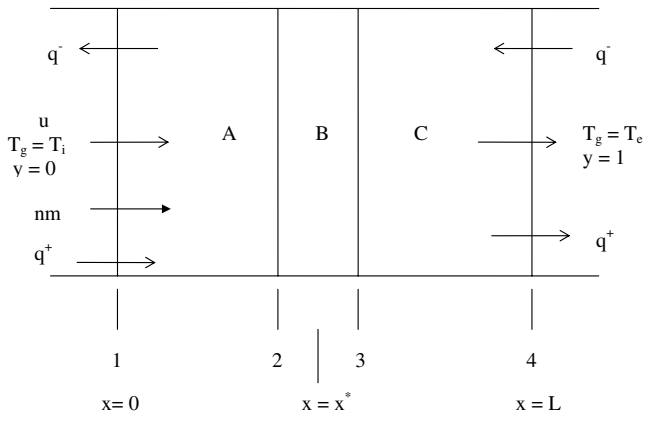

Fig. 1. Schematic diagram of a combustion system in a porous medium.

and the air flow is laminar, the flow may be assumed to be of plug flow nature. For isothermal plug flow of pulverized char particle, the complete burnout time for carbon particles of average size, 100 nm (with 100% carbon content) at stoichiometric dust concentration in air, has been estimated [31] to be about 6×10^{-4} seconds using effective rate constant (includes both kinetics and diffusion) as 0.5 g/(cm^2 s atm O_2), at 1600 K, carbon density [30] as 2 g/cm^2. For the present system, the reaction thickness with this burnout time is estimated around 0.6 mm. This dimension is smaller or nearly equal to the dimension of cavity for highly porous ceramics [5] and metallic structure [4]. With high permeability and porosity of matrix, the combustion can be realized as if in open flow condition in such a small thickness so that the assumption of constant temperature T_m of reaction zone B is justified.

l) At interface 2, the particle suspension in air at $T_g \leqslant T_A$ when enters the reaction region B instantaneously reaches the reaction peak temperature T_m because of high reaction enthalpy flux. So the interface 2 exchanges radiative enthalpy from reaction region B only through emissive/absorptive interaction between reaction temperature T_m and low temperature ($T_g \leqslant T_A$) of solid matrix and carbon dust.

2.2. Basic equations

Using the above mentioned assumptions, the continuity equations for species, the energy equations for both the gas and solid phases are formulated respectively [4,31,33].

In region A

$$\rho uc(\partial T_g/\partial x) = k_g(\partial^2 T_g/\partial x^2) - h_{gc}(n\pi d^2)(T_g - T_c) - h_{ga}a_s(T_g - T_s) \quad (1)$$

Equation of state:

$$\rho = pM/(RT_g) \quad (2)$$

In A and C regions, the net radiative heat flux, q^* is related to heat fluxes q^+ and q^- in forward and backward directions as

$$q^* = q^+ - q^- \quad (3)$$

$$\partial q^*/\partial x = k_s(\partial^2 T_g/\partial x^2) + h_{gs}a_s(T_g - T_s) \quad (4)$$

Using two-flux gray radiation approximation [33], the equation of transfer for intensity in each hemisphere is integrated over their respective hemispheres to yield forward and backward intensities, i^+ and i^- as

$$\partial i^+/2\partial x = -(\alpha + s)i^+ + si^- + \alpha i_b \quad (5)$$

$$\partial i^-/2\partial x = -(\alpha + s)i^- + si^+ + \alpha i_b \quad (6)$$

where

$\alpha = a^*$ or $a^{*\prime}$, $s = s_1$ or s_2, i_b = black body intensity

As each intensity over their respective hemisphere is constant under the two-flux model, the Eqs. (5) and (6) are integrated over each hemisphere to yield

$$\partial q^+/2\partial x = -(\alpha + s)i^+ + si^- + \alpha\sigma T_s^4 \quad (7)$$

$$\partial q^-/2\partial x = -(\alpha + s)i^- + si^+ + \alpha\sigma T_s^4 \quad (8)$$

In region C, $\alpha = a^*$, whereas in region A, $\alpha = a^{*\prime} = ba^*$, where b is the enhancement factor of a^* for presence of carbon particles in the matrix void.

At the interface 2, the absorptance of solid phase and carbon particles at temperature T_2 for incident black radiation of reaction temperature T_m is equal to the emittance of the surface at T_m for electrical nonconductors such as ceramics, metal oxides and poor conductor carbon particles in which the monochromatic emittance is independent of temperature [34].

$$\text{At } x = x_2 : q^- = E^*\sigma T_m^4 - \lambda E^*\sigma T_m^4 \quad (9)$$

where λ is the ratio of cross sectional area of solid with and without suspended carbon particles.

Other boundary conditions are

$$\begin{aligned} &x = 0 && : T_g = T_i, && q^+ = 0 \\ &x = x_2 - \Delta x && : T_g \leqslant T_A, && y = 0 \quad \Delta x \to 0 \\ &x = x_2 && : y = 0, && T_g = T_m \\ &x = x_3 && : y = 1, && T_g = T_m \\ &x = L && : T_g = T_e, && q^- = 0 \end{aligned} \quad (10)$$

These equations are transformed into dimensionless form using following dimensionless quantities:

$$X^* = x^*/L, \quad T^* = (T_g - T_i)/T_i, \quad M_1 = \rho uc/(\sigma T_i^3),$$
$$M_2 = k_s/(\sigma T_i^3 L), \quad M_2 = k_g/(\sigma T_i^3 L) \quad (11)$$

The energy balance of the reaction region B is worked out by considering the total reaction release rate, sensible enthalpy flux of gas and radiative energy flux at 2 and 3 ends. The overall energy balance is made by equating the total reaction heat release rate to sensible enthalpy flux at downstream end, radiation losses at upstream and downstream ends. Heat conductive energy fluxes at both ends of porous medium are assumed to be negligible [3].

2.3. Numerical solutions

The governing differential equations with boundary conditions were numerically integrated using collocation [35]. In this method, the differential equations are converted to nonlinear system of equations with assumed polynomial spatial profiles for temperature and heat fluxes. These algebraic equations were solved using computer. The base line data are as follows:

$$Q' = 1 \times 10^4, \quad T_i = 298 \text{ K}, \quad f = 1, \quad L = 0.1 \text{ m}, \quad s = 0,$$
$$\varphi = 0.95, \quad C = 1.105 \text{ kJ/kg/K}, \quad k_g = 0.078 \text{ W/m/K},$$
$$k_s = 0.18 \text{ W/m/K}, \quad E^* = 0.4$$

The value of $h_{gs}a_s$ is estimated [4] to be 2×10^7 W/m^3/K. The particle size d of carbon black (natural gas) is taken [28] as 40 nm with its carbon content assumed as 100%. The autoignition temperature of carbon black, T_A is taken [32] as 591 K. For suspended coal dust ($d = 10$ μ) in air with stoichiometric dust concentration at finite ignition distance of 5 cm, the laminar burning velocity (u_f) is experimentally determined [36] to be 0.8 m/s. For fine carbon particles, h_{gc} is estimated [31] using Nusselt number as 2.

3. Results and discussion

The temperature of gas, solid matrix and carbon particles coincide due to firstly, high values of $h_{gs}a_s$ imposed [4,5], secondly high value of h_{gc} in region A. With peak temperature above 1600 K, the assumption of constant reaction temperature (T_m) is satisfied. The temperature profiles as a function of X inside the porous medium at different effective absorption coefficient of region A are shown in Fig. 2 with flame position $X^* = 0.5$. In the preheating region A, air temperature T_g remains constant from $x = 0$ to $x = x'$. At $x = x'$, air temperature just increases above T_i and its value has been arbitrarily fixed at $1.01T_i$ i.e. $T^* = 0.01$. Here L', the preheating temperature zone length, $(x^* - x')/L$ is defined as the axial distance between $x = x^*$ and $x = x'$ where $T^* = 0.01$ at $x = x'$. In this system for $b = 1, 2, 4$ and 7.5, the corresponding values of L' are 0.45, 0.35, 0.22 and 0.13, respectively. In the preheating region A, the increase in loading of carbon particles in air stream leads to increase of effective absorption coefficient of the matrix void. So the shorter distance from the combustion zone $x = x_2$), as indicated by L' value, is required for air preheating from T_i to T_A when the carbon particle concentration in the air stream is increased. It can be seen that the change in the effective absorption coefficient of matrix void in preheating region A does not change the interfacial temperature T_A (i.e. $T_A^* = 0.983$). Computational data shows that the variation of $a^{*\prime}$ with same a^* does not change peak temperature T_m and radiative efficiencies (E', E''). This means the presence of carbon particles in region A does not affect the post combustion temperature history and radiative activities as well as the upstream radiative loss. It is as if a single phase gas combustion where $a^* = a^{*\prime}$ as regards the reaction the reaction temperature and radiative output. As such while analyzing the other effects of variables on the system discussed later, the effect $a^{*\prime}$ on the system is assumed to be absent. Fig. 3 shows the absorption coefficient of matrix structure (a^*) on the reaction temperature ($T^{*\prime}$), burning velocity (V^*), and radiative efficiencies (E', E''). As the absorption coefficient (a^*) increases, the radiative energy feedback from the post-flame region to the reaction zone increases. But due to increase in a^*, the increase in radiative energy feedback is partially neutralized with increase in radiative output at both upstream and downstream ends. This combined effect results in only marginal increase in reaction temperature ($T^{*\prime}$) and burning velocity (V^*). At $a^* = 15$, there is no upstream loss. With increase in a^* from 15 to 40, the upstream loss sharply increases. At $a^* > 40$, both upstream and downstream losses increase marginally with increase in a^*.

For combustion of single phase gaseous mixture containing hydrocarbon and air, flame can be stabilized [3,4,37] at any position of X (i.e. X^*) inside the porous system. Assuming similar possibility of stabilization for this system at any value of X^*, the effect of X^* has been analyzed in Fig. 4. The value of $T^{*\prime}$ and V^* are nearly constant for X^* in the range 0.1–0.8. At $X^* > 0.8$, the value of $T^{*\prime}$

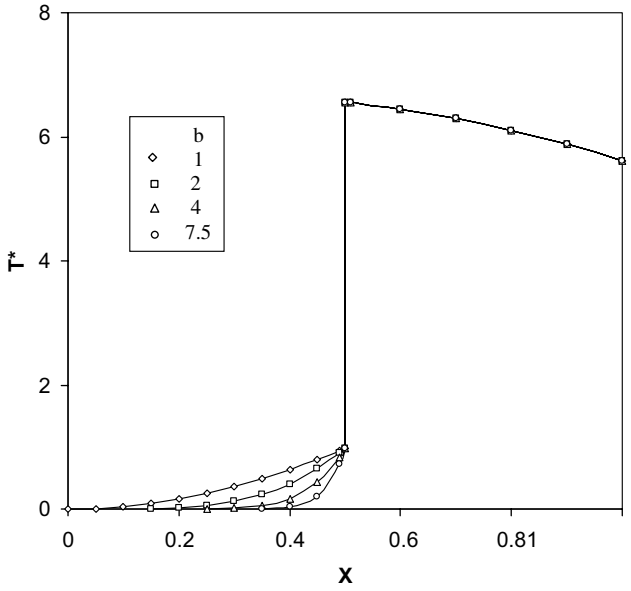

Fig. 2. Effect of effective absorption coefficient of the precombustion zone on the temperature distribution for $X^* = 0.5$, $a^* = 20$ (1/m).

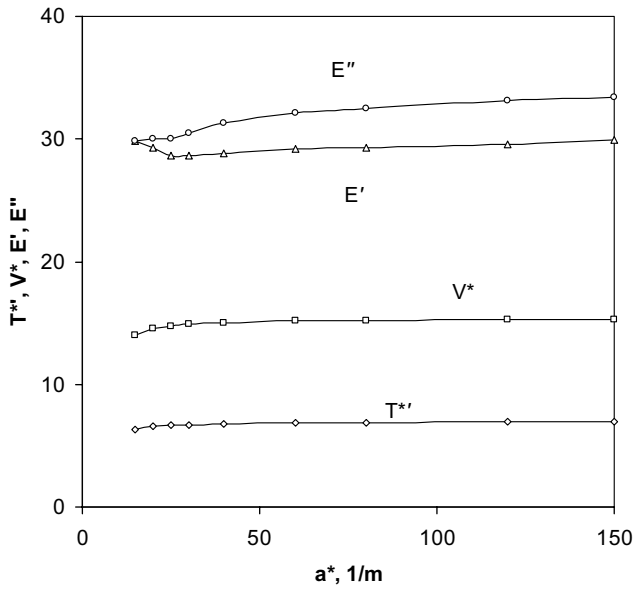

Fig. 3. Effect of absorption coefficient of porous medium on the peak gas temperature, burning velocity and radiative output for $X^* = 0.5$.

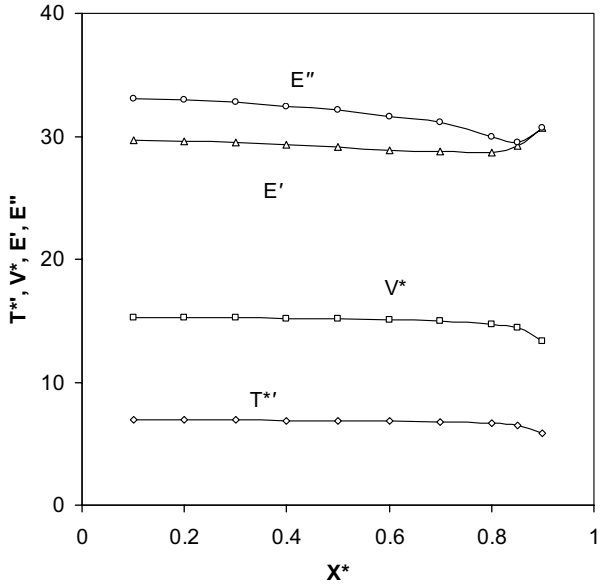

Fig. 4. Effect of position of reaction zone on peak gas temperature, burning velocity and radiative output for $a^* = 60$ (1/m).

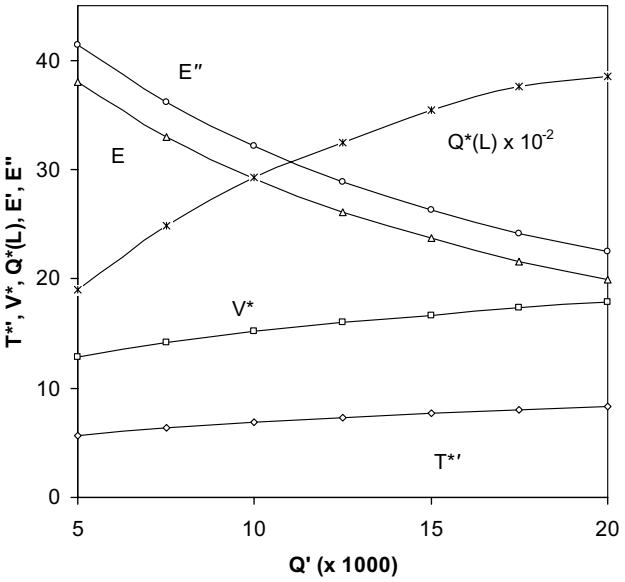

Fig. 6. Effect of reaction heat flux on peak gas temperature, burning velocity and radiative output for $a^* = 60$ (1/m), $X^* = 0.5$.

and V^* decrease sharply with increase in X^*. In porous medium, the radiative heat feedback depends on the value of $T^{*\prime}$, V^* and effective upstream optical thickness. As the position of flame plane (X^*) shifts towards the upstream end, the upstream radiation end loss rises whereas the downstream end loss remains nearly constant for $X^* \leqslant 0.8$. With $X^* > 0.8$, the upstream and downstream losses sharply decrease and increase respectively with increase in x^*. At $X^* = 0.85$, the upstream loss becomes zero. Similar observation has been made earlier [12].

The effect of effective emissivity (E^*) of the porous medium on its thermal performance is presented in Fig. 5. The effect of E^* and a^* are similar except that E^* affects the performance of the prereaction region A, whereas a^* affects that of the whole medium. Accordingly, the effect of E^* on $T^{*\prime}$ and V^* has similar trend. The values of $T^{*\prime}$ and V^* are nearly constant throughout the range of $E^* = 0.2$ to 1.0. However the effect of E^* is significant on E' and E''. At $E^* \leqslant 0.3$, there is no upstream radiative loss. But at $E^* > 0.3$, upstream and downstream radiative losses increase and decrease respectively almost linearly with increase in E^*. Similar trend in the effect of E^* on E' and E'' has been reported earlier [12,19].

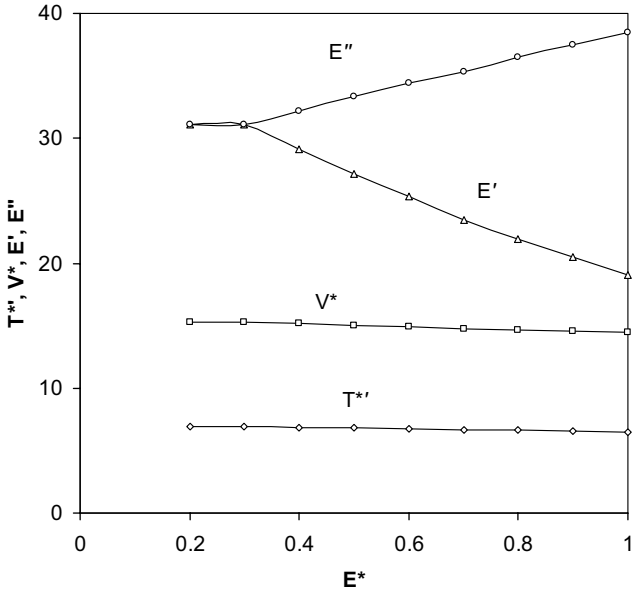

Fig. 5. Effect of emissivity of porous medium on peak gas temperature, burning velocity and radiative output for $a^* = 60$ (1/m), $X^* = 0.5$.

Fig. 6 shows the effect of reaction enthalpy flux, Q' on thermal performance of the system. Both reaction temperature ($T^{*\prime}$) and burning velocity (V^*) increase almost linearly with increase in Q'. With increase in Q', the downstream radiative loss increases but both efficiencies E' and E'' decrease. At low values of Q', the radiative efficiencies are very high. It shows that at low gas flow rate, the conversion of sensible heat of gas to radiative heat becomes more efficient, whereas at high gas flow rate i.e. at high values of Q', the sensible heat loss in exit gas predominates over the radiative heat conversion.

4. Conclusion

In porous medium, the combustion of suspended submicron carbon (carbon black) particles in air is similar to premixed single phase gaseous combustion except the former has shorter length of preheating temperature zone. The absorption coefficient, flame position and emissivity of the porous medium play important role in determining radiative end losses. The downstream radiative output is desirable to heat the load in industrial application whereas the upstream radiative loss is undesirable and a waste. Lower value of absorption coefficient and emissivity of

medium ensure higher downstream radiative output. Also flame position nearer to downstream end increases downstream radiative output. Usual material of construction of porous medium is ceramics i.e. Al_2O_3 or ZrO_2 which has low emissivity (E^*) of 0.28 and 0.31, respectively at 2000 K [2]. Porous ceramic foam with very high porosity is having low absorption coefficient [7,14]. So use of highly porous matrix made of Al_2O_3 or ZrO_2 with flame position stabilized nearer to downstream end will maximize the downstream radiative output with minimum radiative output loss.

Acknowledgements

The authors express their sincere gratitude to Dr. H. S. Maiti, Director, CGCRI for his keen interest and encouragement in this work under the Institute project and kind permission to publish this paper.

References

[1] R. Echigo, Effective energy conversion method between gas enthalpy and gas radiation and application to industrial furnaces, in: Proceedings of the Seventh International Heat Transfer Conference, München, 1982, pp. 361–366.
[2] S. Mößbauer, O. Pickenäcker, K. Pickenäcker, D. Trimis, Application of porous burner technology in energy and heat engineering, in: Proceedings of the Fifth International Conference on Technology and Combustion for a Clean Environment (Clean Air V), 1999, pp. 12–15.
[3] Y. Yoshizawa, K. Sasaki, R. Echigo, Analytical study of structure of radiation controlled flame, Int. J. Heat Mass Transfer 31 (1988) 311–319.
[4] S.B. Sathe, R.E. Peck, T.W. Tong, A numerical analysis of heat transfer and combustion in porous radiant burners, Int. J. Heat Mass Transfer 33 (6) (1990) 1331–1338.
[5] P.F. Hsu, J.R. Howell, R.D. Mathews, A numerical investigation of premixed combustion within porous media, Trans. ASME, J. Heat Transfer 115 (1993) 744–750.
[6] D. Trimis, F. Durst, O. Pickenäcker, K. Pickenäcker, Porous medium combustion versus combustion systems with free flame, in: Proceedings of the Second International Symposium on Heat Transfer Enhancement and Energy Conservation, Guangzhou, China, 1997.
[7] A.J. Barra, J.L. Ellzey, Heat recirculation and heat transfer in porous burners, Combust. Flame 137 (2004) 230–241.
[8] M. Kapalan, M.J. Hall, The combustion of liquid fuels within a porous media radiant burner, Exp. Therm. Fluid Sci. 11 (1) (1995) 13–20.
[9] F. Durst, M. Keppler, M. Weclas, Air-assisted nozzle applied to very compact, ultra-low emission porous medium oil-burner, in: Proceedings of the Third Workshop (Spary 97), Lampoldshausen, 1997.
[10] J.R. Howell, M.J. Hall, J.L. Ellzey, Combustion of hydrocarbon within porous inert media, Prog. Energ. Combust. Sci. 22 (1996) 121–145.
[11] C.-J. Tseng, J.R. Howell, Combustion in liquid fuels in porous radiant burner, Combust. Sci. Technol. 112 (1996) 141–161.
[12] T.K. Kayal, M. Chakravarty, Combustion of liquid fuel inside inert porous media: an analytical approach, Int. J. Heat Mass Transfer 48 (2005) 331–339.
[13] V.V. Martnenco, R. Echigo, H. Yoshida, Mathematical model of self-sustaining combustion in inert porous medium with phase change under complex heat transfer, Int. J. Heat Mass Transfer 41 (1) (1998) 117–126.
[14] T. Fuse, Y. Araki, K. Kobayashi, M. Hasatani, Combustion characteristics in oil-vaporizing sustained by radiant heat flux enhanced with higher porous ceramics, Fuel 82 (11) (2003) 1411–1417.
[15] T.K. kayal, M. Chakravarty, Modeling of a conceptual self-sustained liquid vaporization-combustion system with radiative output using inert porous media, Int. J. Heat Mass Transfer 50 (2007) 1715–1722.
[16] H. Takami, T. Suzuki, Y. Itaya, M. Hasatani, Performance of flammability of kerosene and NO_x emission in porous burner, Fuel 77 (3) (1998) 165–171.
[17] S. Jugjai, N. Wongpanit, T. Laoketkan, S. Nokkaew, The combustion of liquid fuels using a porous medium, Exp. Therm. Fluid Sci. 26 (1) (2002) 15–23.
[18] S. Jugjai, N. Polmart, Enhancement of evaporation and combustion of liquid fuels through porous media, Exp. Therm. Fluid Sci. 27 (8) (2003) 901–909.
[19] T.K. Kayal, M. Chakravarty, Modeling of trickle flow liquid fuel combustion in inert porous medium, Int. J. Heat Mass Transfer 49 (5–6) (2006) 975–983.
[20] L.D. Smoot, P.J. Smith, Coal Combustion and Gasification, Plenum Press, New York, 1985.
[21] T. Abbas, P.G. Costen, F.C. Lockwood, Solid fuel utilization: from coal to biomass, in: Proceedings of the 26th Symposium (International) on Combustion, Combustion Institute, Pitsburg, 1996, pp. 3041–3058.
[22] F. Scala, R. Chirone, Fluidized bed combustion of alternative solid fuels, Exp. Therm. Fluid Sci. 28 (7) (2004) 691–699.
[23] K. Suksakraisorn, S. Palumsawad, P. Vallikul, B. Fungtammasan, A. Accary, Co-combustion of municipal solid waste and Thai lignite in a fluidized bed, Energ. Conv. Manage. 45 (6) (2004) 947–962.
[24] Y. Hua, G. Flamant, J. Lu, D. Gauthier, Modeling of axial and radial solid segregation in a CFB boiler, Chem. Eng. Process. 43 (8) (2004) 971–978.
[25] D.J. Dimitriou, N. Kandamby, F.C. Lockwood, A mathematical modeling technique for gaseous and solid fuel reburning in pulverized coal combustors, Fuel 82 (15–17) (2003) 2107–2114.
[26] P.F. Hsu, W.D. Evans, J.R. Howell, Experimental and mathematical study of premixed combustion within nonhomogeneous porous ceramics, Combust. Sci. Technol. 90 (1993) 149–172.
[27] H. Yoshida, J.H. Yun, R. Echigo, T. Tomimura, Transient characteristics of combined conduction, convection and radiation heat transfer in porous media, Int. J. Heat Mass Transfer 33 (5) (1990) 847–857.
[28] E.M. Dannenberg, in: M. Grayson (Ed.), Encyclopedia Chem. Technol., third ed., vol. 4, John Wiley, New York, 1978, p. 652.
[29] W. Strauss, Industrial Gas Cleaning, Pergamon Press, London, 1966, p. 219.
[30] P.J. Schneider, Conduction, in: W.M. Rohsenow, J.P. Hartnett (Eds.), Handbook of Heat Transfer, McGraw-Hill, New York, 1973, pp. 3–37.
[31] G.L. Borman, K.W. Ragland, Combustion Engineering, McGraw-Hill, New York, 1998, p. 473, 516.
[32] C.L. Mantell, Industrial Carbon, second ed., D. Van Nostrand, New York, 1946, p. 420, 427.
[33] S.W. Baek, The premixed flame in a radiatively active porous medium, Combust. Sci. Technol. 64 (1989) 277–287.
[34] E.R.G. Eckert, R.M. Drake Jr., Analysis of Heat and Mass Transfer, McGraw-Hill, New York, 1972, p. 612.
[35] P. Razelos, Methods of obtaining approximate solutions, in: W.M. Rohsenow, J.P. Harnetts (Eds.), Handbook of Heat Transfer, McGraw-Hill, New York, 1973, pp. 4–72.
[36] R.H. Essenhigh, J. Csaba, The thermal radiation theory for plane flame propagation in coal dust clouds, Proceedings of the Ninth Symposium (International) on Combustion, Cornell University, Combustion Institute, 1962, pp. 111–125.
[37] Y. Kotani, T. Tokeno, An experimental study on stability and combustion characteristics of excess enthalpy flame, Proceedings of the 19th Symposium on Combustion, The combustion Institute, 1982, pp. 1503–1509.